THE JOURNAL OF BIOLOGICAL CHEMISTRY
Vol. 278, No. 18, Issue of May 2, pp. 16336–16346, 2003
Printed in U.S.A.

Subcellular Localization and *in Vivo* Subunit Interactions of Ubiquitous μ-Calpain*

Received for publication, August 23, 2002, and in revised form, January 15, 2003
Published, JBC Papers in Press, February 18, 2003, DOI 10.1074/jbc.M208657200

Shirley Gil-Parrado‡§¶, Oliver Popp‡, Tobias A. Knoch‖, Stefan Zahler, Felix Bestvater‖, Marcel Felgenträger‡, Andreas Holloschi‡‡, Amaury Fernández-Montalván‡, Ennes A. Auerswald‡§§, Hans Fritz‡, Pablo Fuentes-Prior¶¶, Werner Machleidt§, and Eberhard Spiess‖**

*From the ‡Abteilung für Klinische Chemie und Klinische Biochemie, Chirurgische Klinik Innenstadt, Klinikum der Ludwig-Maximilians-Universität, D-80336 München, §Adolf-Butenandt-Institut der Ludwig-Maximilians-Universität, D-80336 München, ‖Deutsches Krebsforschungszentrum, D-69120 Heidelberg, **Physiologisches Institut der Ludwig-Maximilians-Universität, D-80336 München, ‡‡Institut für Molekularbiologie und Zellkulturtechnik, Fachhochschule Mannheim, D-68163 Mannheim, and ¶¶Max-Planck-Institut für Biochemie, D-82152 Martinsried, Germany*

Ubiquitously expressed calpains are Ca^{2+}-dependent, intracellular cysteine proteases comprising a large catalytic subunit (domains DI–DIV) and a noncovalently bound small regulatory subunit (domains DV and DVI). It is unclear whether Ca^{2+}-induced calpain activation is followed by subunit dissociation or not. Here, we have applied advanced fluorescence microscopy techniques to study calpain subunit interactions in living cells using recombinant calpain subunits or domains fused to enhanced cyan and enhanced yellow fluorescent reporter proteins. All of the overexpressed variants of the catalytic subunit (DI-IV, DI-III, and DI-IIb) were active and Ca^{2+}-dependent. The intact large subunit, but not its truncated variants, associates with the small subunit under resting and ionomycin-activated conditions. All of the variants were localized in cytoplasm and nuclei, except DI-IIb, which accumulates in the nucleus and in nucleoli as shown by microscopy and cell fractionation. Localization studies with mutated and chimeric variants indicate that nuclear targeting of the DI-IIb variant is conferred by the two N-terminal helices of DI. Only those variants that contain DIII migrated to membranes upon the addition of ionomycin, suggesting that DIII is essential for membrane targeting. We propose that intracellular localization and in particular membrane targeting of activated calpain, but not dissociation of its intact subunits, contribute to regulate its proteolytic activity *in vivo*.

Calpains are intracellular cysteine endopeptidases (clan CA) requiring Ca^{2+} ions for activity. The family members can be classified as typical calpains, which are further divided into ubiquitous and tissue-specific calpains, and atypical calpains (reviewed in Ref. 1). Ubiquitous calpains are heterodimers (molecular mass, ~110 kDa) made up of a catalytic (molecular mass, ~80 kDa; 80K) and a common regulatory (molecular mass, ~30 kDa; 30K) subunit (2, 3). Two calpain isoforms are known that share about 62% identical residues of their catalytic subunits but differ in the Ca^{2+} concentrations required for activation *in vitro*; although μ-calpain is activated by 5–50 μM Ca^{2+}, m-calpain requires 0.2–1 mM Ca^{2+} concentrations for activation (4). Calpain activity is regulated *in vivo* by phosphorylation (5) and by the endogenous intracellular inhibitor, calpastatin (6). The latter are widely distributed heat-stable proteins acting specifically on calpains *in vitro* in the presence of Ca^{2+} (7). In addition, calpain inhibition by kininogen domain II (8) and growth arrest-specific factor 2 (9) has been reported.

Upon exposure to Ca^{2+}, ubiquitous calpains undergo *in vitro* limited autolysis of both subunits, which reduces Ca^{2+} requirement for activity (10). Following initial autolysis at the N terminus of both subunits, further degradation of the large subunit eventually leads to a loss of enzymatic activity (11). Controversial hypotheses of the activation mechanism of calpain *in vivo* and the role of Ca^{2+} in this process have been presented (1, 11, 12). Important open questions in this regard are whether or not calpain activation results in dissociation of the large and small subunits and the probable role of autolysis.

Recent crystal structures of full-length, Ca^{2+}-free rat and human m-calpain (13, 14) confirmed that the catalytic subunit is organized in four domains, termed DI–DIV; the 30K subunit consists of domains DV and DVI (Fig. 1, *A* and *F*). Compared with the structurally homologous papain, subdomains DIIa and DIIb are misplaced, with catalytic residues Cys^{105} and His^{262} located about 10 Å apart. Moreover, the substrate binding cleft is disrupted and open, which is incompatible with productive binding of peptide substrates. These features explain the inactivity of calpains in the absence of Ca^{2+}. The crystal structure of Ca^{2+}-bound DII domain discloses two Ca^{2+} ions that bridge subdomains IIa and IIb[1] to form the catalytically competent active site, highlighting an important effect of calcium for calpain activity (15). There are, however, additional Ca^{2+}-binding sites with important roles for activity.

Domains DIV and DVI contain five EF hand motifs highly similar to those of the major intracellular Ca^{2+}-binding protein, calmodulin. Accordingly, the first three N-terminal EF

* This work was supported by Grants A3 (to E. A. A.) and A6 (to W. M.) from the Sonderforschungsbereich 469 of the Ludwig-Maximilians-Universität München. The costs of publication of this article were defrayed in part by the payment of page charges. This article must therefore be hereby marked "*advertisement*" in accordance with 18 U.S.C. Section 1734 solely to indicate this fact.

¶ Supported by a research fellowship from the Deutschen Akademischen Austauschdienst. To whom correspondence should be addressed: Abteilung für Klinische Chemie und Klinische Biochemie, Chirurgische Klinik Innenstadt, Klinikum der Ludwig-Maximilians-Universität, Nussbaumstrasse 20, D-80336 München, Germany. Tel.: 49-89-51602679; Fax: 49-89-51604740; E-mail: shirgilpa@web.de.

§§ Present address: Neurologische Klinik und Poliklinik Grosshadern, Klinikum der Ludwig-Maximilians-Universität, D-81377 München, Germany.

[1] We follow the domain nomenclature proposed by Strobl *et al.* (14), illustrated in Fig. 1*A*. In this nomenclature, the papain-like catalytic domain DII is further subdivided into two subdomains, DIIa and DIIb.

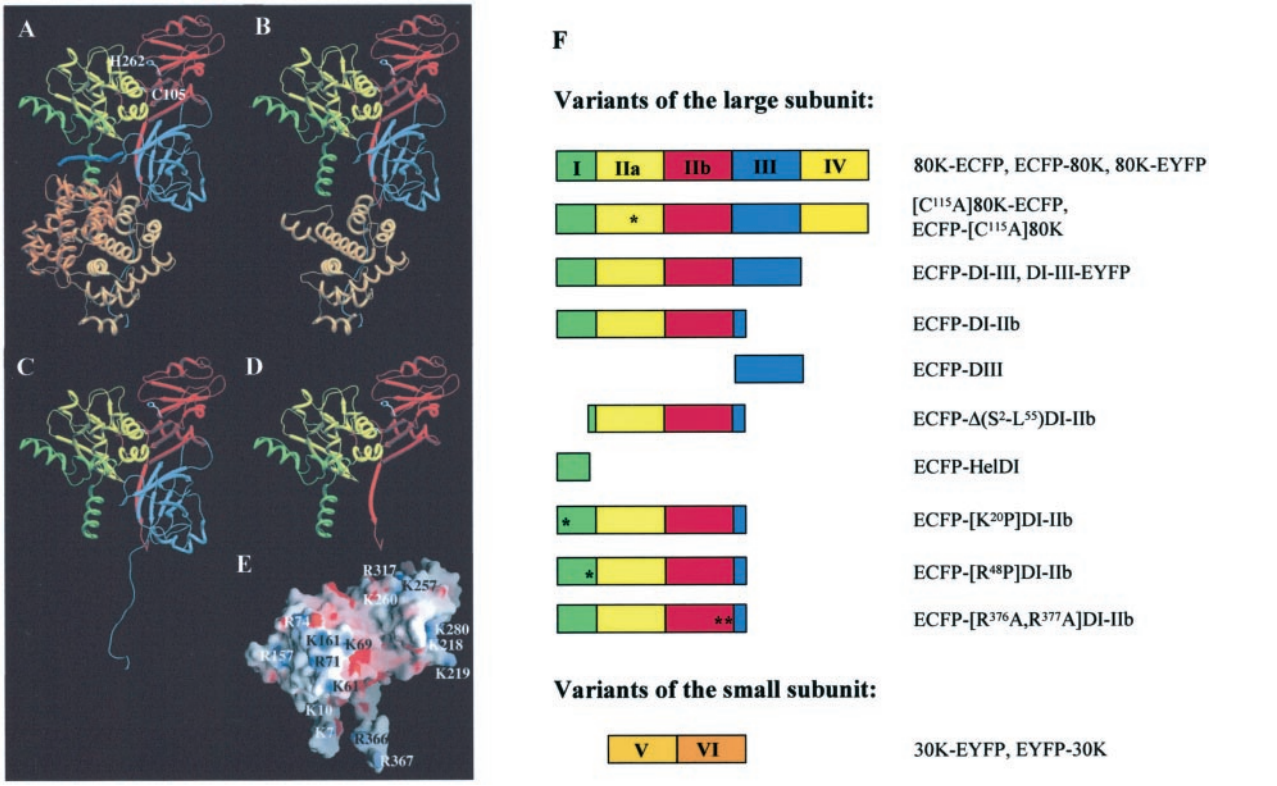

FIG. 1. **Calpain variants used in subcellular localization and subunit interaction studies.** *A–D*, ribbon drawings of m-calpain three-dimensional structure and variants studied in this work. *B*, 80K; *C*, DI-III; *D*, DI-IIb. The panels were prepared with SETOR using the Protein Data Bank entry for human m-calpain (1DKV). Color labels of the domains are as follows: I, *green*; IIa, *yellow*; IIb, *red*; III, *blue*; IV, *gold-brown*; V, *orange-brown*; and VI, *orange*. *E*, electrostatic surface potential of DI-IIb calculated with the GRASP software. Positively and negatively charged surfaces are *blue* and *red* colored, respectively. *F*, summary of variants of human μ-calpain overexpressed in COS 7 and LCLC 103H cells. The *asterisks* indicate the positions of mutated amino acid residues.

hands bind Ca^{2+} (16). Calcium-mediated calpain activation was therefore proposed to result from Ca^{2+} binding to these domains, mainly to the third EF hand in DIV. Ion binding is expected to promote release of the N-terminal α-helix that anchors the catalytic and regulatory subunit, with concomitant displacement of DIIa toward DIIb (17). An alternative hypothesis points up the role of the synaptotagmin C2-like domain DIII, which harbors several acidic residues within a prominent solvent-exposed loop. This "acidic loop" is spatially adjacent to DIIb and engages in electrostatic interactions with the latter (14). It was suggested, therefore, that Ca^{2+} binding to this loop could release subdomain IIb to move toward IIa, thus allowing formation of a functional catalytic center (the "electrostatic switch" hypothesis). Furthermore, it was proposed that the Ca^{2+} coordination spheres might be only incompletely formed by protein oxygen atoms and that additional ligands provided by negatively charged head groups of acidic phospholipids complete these coordination spheres. Indeed, acidic phospholipids such as phosphorylated phosphatidyl inositols reduce the Ca^{2+} concentration required for autolysis *in vitro* (10, 18, 19), and mutation of the acidic residue Glu^{504} of m-calpain significantly affects Ca^{2+} sensitivity of the enzyme (13). Finally, DIII alone binds Ca^{2+} with an affinity comparable with that of DIV, which is increased 2–10-fold upon the addition of liposomes (20). Conversely, Ca^{2+} significantly promotes phospholipid binding in a similar manner as observed with the C2 synaptotagmin domain. These findings suggest a connection between calpain activation and membrane translocation (see *e.g.* Ref. 21).

In the light of these findings, we have decided to study subcellular localization and subunit interactions of endogenous calpains and overexpressed human μ-calpain subunits and several engineered variants thereof, aiming to provide insight into the calpain activation mechanism *in vivo*. Firstly, we have followed the subcellular distribution of endogenous ubiquitous human calpains and calpastatin under resting and Ca^{2+}-activated (ionomycin-induced) conditions. Next, we have overexpressed the active 80K subunit of human μ-calpain and its truncated variants DI-III, DI-IIb, and DIII, N- or C-terminally fused to ECFP,[2] in COS 7 and in LCLC 103H cells. Co-expression with 30K chimeras that incorporate EYFP allowed us to analyze the interactions between the 80K and 30K subunits *in vivo* using fluorescence energy transfer techniques (FRET). This technique is particularly suited to demonstrate intimate (below 80 nm) contact between reaction partners. Recent progress in fluorescence microscopy has made it possible to apply this technique to interaction analysis in living cells (22). At the same time, overexpression of the 80K-EYFP chimera in cells stably overexpressing a membrane marker, mem-ECFP, combined with co-localization analysis (23) supported the membrane association of this subunit. We provide evidence against dissociation of calpain subunits upon activation *in vivo*. Both endogenous and overexpressed calpain variants were localized in the cytoplasm and/or nucleus of cells, respectively, except DI-IIb, which accumulated in the nucleus and even in nucleoli. Localization studies with five additional truncated or mutant variants of the DI-IIb construct identify the N-terminal helices of DI as a putative nuclear-targeting motif.

[2] The abbreviations used are: ECFP, enhanced cyan fluorescent protein; AC27P, acetyl calpastatin 27-peptide; EYFP, enhanced yellow fluorescent protein; FRET, fluorescence resonance energy transfer; Suc-LLVY-amc, succinyl-Leu-Leu-Val-Tyr-7-amino-4-methylcoumarin.

TABLE I
Primers used for the construction of large and small subunit variants of human μ-calpain fused to ECFP and EYFP

Primer[a]	Sequence	Variant
Forward primers		
*Eco*RI 80K	5′-CCG *GAA TTC* TGA TGT CGG AGG AGA TC-3′	80K-ECFP, 80K-EYFP, [C115A]80K-ECFP, ECFP-DI-III, DI-III-EYFP
*Hin*dIII_DIII	5′-CCC *AAG CTT* CGA TGA TCC GCA AAT GGA ACA CCA-3′	ECFP-DIII
*Bgl*II_30K	5′-GGA *AGA TCT* ATG TTC CTG GTT AAC TCG TTC-3′	30K-EYFP
Reverse primers		
*Bam*HI_80K	5′-CGC *GGA TCC* TGC AAA CAT GGT CAG CTG-3′	80K-ECFP, 80K-EYFP, [C115A]80K-ECFP
*Bam*HI_DIII	5′-CGC *GGA TCC* TCA TTA CTG GTC ATC CAG CTC CAC AGT-3′	ECFP-DI-III, DI-III-EYFP, ECFP-DIII
*Sma*I_30KHis	5′-*CCC CGG G*AG TGA TGA TGA TGA TGA TGG GAA TAC ATA GTC AGC TGC AG-3′	30K-EYFP

[a] The name of the primer includes the DNA restriction enzyme used for cloning (in italics). The corresponding cleavage sites are also in italics.

EXPERIMENTAL PROCEDURES

Materials—The plasmid vectors pECFP-C1, pECFP-N1, pEYFP-C1, and pEYFP-N1 were purchased from Clontech; restriction endonucleases and DNA modifying enzymes were from Roche Biochemicals and New England Biolabs. Antibodies anti-peptide 80K and anti-peptide 76K were produced by Biogenes on request. Commercially available antibodies used were anti-DII (804–051-R100, Alexis), anti-80K (MAB3104, Chemicon), anti-30K (MAB3083, Chemicon), anti-calpastatin (MA3–945, ABR), anti-living colors (8367–1, Clontech), and anti-calpain (laboratory stock). The fluorogenic substrate Suc-LLVY-amc was purchased from Bachem. The calpain inhibitor, AC27P, and ionomycin were from Sigma. All other reagents were of the highest purity commercially available.

Plasmid Construction and Preparation—All of the variants of human μ-calpain large subunit for expression in mammalian cells were constructed using as scaffold a self-prepared semi-synthetic gene, pUC18_80K DNA, or a variant thereof with the active site residue Cys^{115} mutated to alanine (pUC18_ [C115A]80K).[3] Variants DI-IV (Ser^{2}–Ala^{711}), DI-III (Ser^{2}–Asp^{523}), and DIII (Ile^{363}–Gln^{527}) were obtained via PCR, using primers listed in Table I. The DNA for variant DI-IIb (Ser^{2}–Thr^{390}) was obtained by digestion of pECFP_80K DNA with the restriction enzymes *Eco*RI and *Sac*II. The small subunit DNA was amplified via PCR using as template a plasmid coding for the His-tagged 30K subunit[3] (Table I). The DNA fragments were subcloned into the appropriate vectors, pECFP-N1 (80K-ECFP, [C115A]80K-ECFP), pECFP-C1 (ECFP-80K, ECFP-[C115A]80K, ECFP-DI-III, ECFP-DI-IIb, ECFP-DIII), pEYFP-N1 (30K-EYFP, 80K-EYFP, DI-III-EYFP), and pEYFP-C1 (EYFP-30K), after digestion with the indicated restriction enzymes (Table I). Competent TG1 cells were transformed with the ligation mixtures, and the resulting isolated plasmids with the correct sequences were used for further transfections. The variants ECFP-[K20P]DI-IIb, ECFP-[R48P]DI-IIb, and ECFP-[R376A,R377A]-DI-IIb were prepared via PCR using as template pECFP_DI-IIb DNA according to the QuikChange™ site-directed mutagenesis kit instructions (Stratagene) using the primers listed in Table II. Variants that either lack the two N-terminal helices (ECFP-Δ(Ser^{2}–Leu^{55})DI-IIb) or consist of these two helices fused to ECFP (ECFP-(Ser^{2}–Leu^{55})) were obtained by double-digesting pECFP_DI-IIb DNA with *Eco*RI/*Kpn*I or *Kpn*I/*Bam*HI, respectively, followed by ligation into pECFP-C1 digested with the same pairs of enzymes. The identity of cloned DNAs was verified by sequencing both DNA strands.

Cell Culture and Transfection—For routine cell culture RPMI 1640 medium (LCLC 103H cells, DSMZ ACC 384) or Dulbecco's modified Eagle's medium (COS 7, ATCC CRL 1651) (Invitrogen) were supplemented with 10% fetal calf serum (Sigma), 0.6% L-glutamine (Invitrogen). Transfection was carried out using the FuGENE 6 Reagent (Roche Molecular Biochemicals) according to the general protocol suggested by the manufacturer. COS 7 and LCLC 103H cells transiently overexpressing the corresponding construct were used in this study. For membrane targeting studies a LCLC 103H clone constitutively expressing the membrane marker mem-ECFP (Clontech) was transfected with 80K-EYFP and DI-III-EYFP DNAs. For localization experiments of ECFP-DI-IIb and variants thereof, a LCLC 103H clone expressing constitutively histone H2A coupled to EYFP was used. Histone H2A-EYFP and mem-ECFP expressing cell clones of LCLC 103H were obtained as described earlier (24).

[3] D. Pfeiler, I. Assfalg-Machleidt, E. Bonzon, N. Gollmitzer, D. Gabrijelcic-Geiger, J. K. Gerber, H. Fritz, E. A. Auerswald, S. Gil-Parrado, and W. Machleidt, manuscript in preparation.

Isolation and Analysis of Cytoplasmic Proteins—Cytoplasmic extracts from approximately 10^{6} cells were prepared according to Ref. 25. Briefly, pools of cells transfected with the corresponding constructs were either kept untreated or incubated with the ionophore for 30 min before cell lysis and fractionation. The protein content was assayed by the bicinchoninic acid method (26). The samples were electrophoretically resolved on SDS-Tris-glycine (12.5%) gels, transferred to nitrocellulose membranes (Schleicher & Schuell), and probed against the indicated antibodies; the resulting complexes were detected with anti-mouse or anti-rabbit horseradish peroxidase-linked IgG from New England Biolabs using ECL (Amersham Pharmacia Biotech).

Immunoprecipitation—The cell lysates were preincubated with the antibody anti-80K, bound to protein G-agarose (Roche Diagnostics), and eluted according to Ref. 12. The immunoprecipitated proteins were separated in SDS-Tris-glycine (12.5%) gels, transferred to nitrocellulose membranes, and detected with anti-calpain, a polyclonal antibody that recognizes both large and small calpain subunits.

Epifluorescence Microscopy—The cells were cultured on 4.2-cm-diameter coverslips (Langenbrinck) or in Lab-Tec™ II cover glass chambers (Nunc) and used for microscopical studies 24–72 h after transfection with the indicated constructs. Prior to observation, the coverslips were mounted in perfusion chamber holders (PeCon) that were kept at 34–36 °C and 5% CO_2 during observation. The microscope (Axiovert S100 TV, Zeiss) was equipped with objectives Fluor 40/1.3 oil Ph2, Apochromat 40/1.2 W korr, or Neofluar 63/1.25 oil Ph3, filter wheels, and shutters (Ludl); Orca 4742–95 CCD camera (Hamamatsu), and controlled by OpenLab software (Improvision). Filter systems for ECFP, EYFP, and FRET were from Chroma Technologies (excitation (Ex): 435/10 nm and 515/10 nm; single band: dichroic mirror $(DM)_{ECFP}$ 455 nm, emission $(Em)_{ECFP}$ 480/40 nm and DM_{EYFP} 530 nm, Em_{EYFP} 560/40 nm; doubleband: DM_{ECFP} 475 nm, Em_{ECFP} 470/30 nm, DM_{EYFP} 556 nm, Em_{EYFP} 555/40 nm; and FRET: DM 460 nm, Em 535/30 nm). All of the observations were carried out in the corresponding growth medium. The images were captured before and after the addition of ionomycin to 2 μM end concentration during 30 min in 5-min intervals. To obtain optical section series a Piezo electric motor (Physical Instruments) was used to drive the C-Apochromat 40× objective in appropriate steps. The images were processed by deconvolution, and false color look-up tables were applied to them for the final presentation. Colocalization was analyzed by the respective Openlab™ software module, which operates on a pixel-by-pixel comparison of pairs of images (23).

Immunocytofluorescence Detection of Endogenous Calpain and Calpastatin—The cells were grown on glass coverslips and stained according to Becton Dickinson Transduction Laboratories protocol using the indicated antibodies. For fluorescence microscopy, the coverslips were mounted on microscope slides with PermaFluor (Immunotech) and inspected in the microscope (LSM 410, Zeiss) equipped with the objective Fluor 63/1.4 oil Ph2. The images were acquired using LSM410 software version 3.95 (Zeiss). For cytoskeletal immunostaining (F-actin), the cells were preincubated with ALEXA633-phalloidin (Molecular Probes). The second antibodies used were ALEXA488 anti-mouse and anti-rabbit (Molecular Probes), detected at excitation 488 nm, beam splitter FT 488/543, and emission 515–525 nm. F-actin was visualized with the same beam splitter at excitation 633 nm and emission >665 nm. The image parameters were 512 × 512 pixels, pinhole 20.

Confocal Laser Scanning Microscopy—The cells were prepared as for epifluorescence microscopy. The microscope (Leica TCS SP) was equipped with objectives, Fluor 40/1.3 oil Ph2 and Neofluar 63/1.25 oil Ph3, and the following filter sets: Ex_{ECFP} 453 nm, Em_{ECFP} 495/60 nm; Ex_{EYFP} 514 nm, Em_{EYFP} 585/70 nm. The images were taken before and

TABLE II
Primers used for the construction of ECFP-DI-IIb variants

Primer	Sequence[a]	Variant
K20_Forward	5′-GCT CAG GTT CAG CCG CAG CGT GCT CGA GAA-3′	K20P
K20_Reverse	5′-TTC TCG AGC ACG CTG CGG CTG AAC CTG AGC-3′	K20P
R48_Forward	5′-GAA CAG CTG CGC GTA CCG TGC CTG CAG TCC-3′	R43P
R48_Reverse	5′-GGA CTG CAG GCA CGG TAC GCG CAG CTG TTC-3′	R43P
R376/377_Forward	5′-TCC CGT ACC ATC GCG GCG TGG AAC ACC ACC-3′	R376A, R377A
R376/377_Reverse	5′-GGT GGT GTT CCA CGC CGC GAT GGT ACG GGA-3′	R376A, R377A

[a] Mutations are underlined.

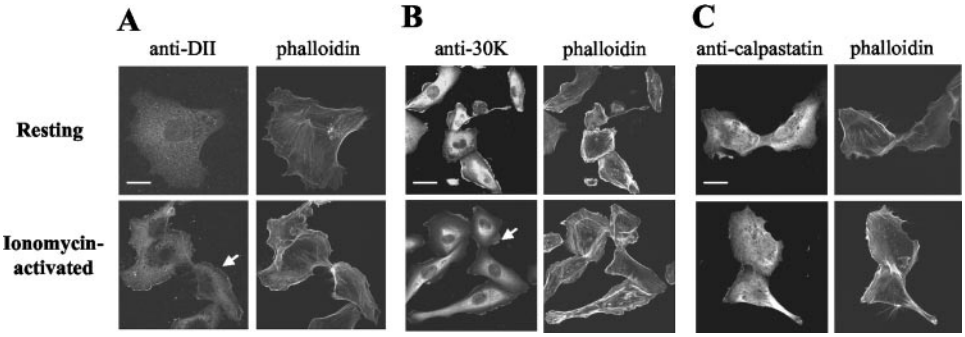

FIG. 2. **Differential subcellular localization of endogenous ubiquitous calpains and calpastatin by immunofluorescence.** The cells were permeated, fixed, and stained as explained under "Experimental Procedures." Confocal laser scanning microscopy images were taken before or after treatment with 2 μM ionomycin as indicated. The cells were preincubated with anti-DII (*A*), anti-30K (*B*), or anti-calpastatin monoclonal antibodies (*C*), as well as with phalloidin (*A–C*) to detect F-actin. Notice the nuclear localization of calpastatin in *C*. The arrows indicate membrane association of the large and small subunit. The *bars* represent 12.5 μm (*A*, *upper panels*), 25 μm (*A*, *lower panels*, and *C*), and 40 μm (*B*).

after the addition of 2 μM ionomycin during 30 min in 5-min intervals. The imaging parameters were 512 × 512 pixels, pinhole 1. Other relevant parameters are given with the respective images. All of the images were processed with a 3 × 3 median filter.

Calpain Activity in Living Cells—Calpain activity in living cells was determined as previously described (27), using the fluorogenic substrate Suc-LLVY-amc. The specificity of calpain cleavage was evaluated by preincubating culture cells with 50 μM AC27P (28) for 1 h before treatment with 2 μM ionomycin.

Measurement of Free Ca^{2+} Concentrations—Free Ca^{2+} concentrations in COS 7 cells were determined before and after the addition of 2 μM of ionomycin, as previously described (27).

RESULTS

Subcellular Localization of Endogenous Calpain and Calpastatin by Immunocytofluorescence—The subcellular localization of endogenous calpain and calpastatin was characterized by immunocytofluorescence microscopy using the monoclonal antibodies anti-DII (specific for μ-calpain large subunit residues Gly^{245}–Phe^{265}), anti-30K, and anti-calpastatin, respectively. Prior to Ca^{2+} mobilization, both calpain subunits and calpastatin are homogenously distributed in the cytoplasm, with a slight preponderance around the nuclear region (Fig. 2). Also, calpastatin accumulated in the nuclei (Fig. 2*C*). After the addition of ionomycin, fluorescence labeling caused by calpain detection increased at cell membranes (Fig. 2, *A* and *B*), whereas calpastatin did not relocalize to membranes under calcium-stimulating conditions (Fig. 2*C*).

Overexpression of ECFP- and EYFP-fused Human μ-Calpain Variants in COS 7 and LCLC 103H Cells—For expression in mammalian cells, DNA fragments coding for the human μ-calpain 80K subunit (residues Ser^2–Ala^{711}) or its truncated variants Ser^2–Asp^{523} (DI-III), Ser^2–Thr^{390} (DI-IIb), and Ile^{363}–Gln^{527} (DIII), as well as the active site mutant [C115A]80K were ligated into vector pECFP-C1 to generate chimeric proteins N-terminally extended with ECFP. DNAs coding for the wild type and active site-mutated large subunit were ligated into pECFP-N1 to produce variants C-terminally tagged with ECFP, respectively. 80K and DI-III were also fused to the N terminus of EYFP. Similarly, the 30K DNA was ligated into pEYFP-C1 or pEYFP-N1 to allow expression of chimeric constructs with EYFP attached to the N or C terminus of the small subunit, respectively (see Fig. 1*F* for a schematic representation of the variants).

First, we determined whether fusion of enhanced fluorescence protein at either terminus of the 80K calpain subunit influences the protein expression level. LCLC 103H cells were transfected with plasmids encoding for either the individual large subunit (pECFP_80K, p80K_ECFP) or small subunit chimeras (p30K_EYFP and pEYFP_30K) or co-transfected with all possible combinations of chimeric 80K and 30K constructs. The cells were lysed 72 h after transfection, and the cytoplasmic extracts were analyzed by Western blot using anti-DII antibody (Fig. 3*A*). All of the variants were successfully overexpressed, but the expression levels of variants in which ECFP is fused to the N terminus of the 80K subunit were systematically lower than those of the C-terminal fusions (Fig. 3*A*). The latter species were therefore selected for subsequent cellular localization studies. Of note, the 80K subunit of endogenous calpain was also detected in mock transfected cells (Fig. 3*A*).

Intracellular Calcium Concentrations in COS 7 and LCLC 103H Cells—Addition of a calcium ionophore to cells leads to an increase in the intracellular calcium concentration with concomitant generation of calpain activity (27, 29). Fura-2 measurements of intracellular calcium concentrations were carried out in living cells before and after addition of 2 μM ionomycin. In both cell lines, the addition of ionomycin caused a fast transient increase ("burst") in the intracellular Ca^{2+} concentration before equilibrium was reached (Fig. 3*B*). Interestingly, we observed remarkable differences regarding (i) the peak values of intracellular Ca^{2+} concentration (between 800 nM and 1.6 μM in LCLC 103H cells (27), but only between 180 and 240 nM in COS 7 cells) and (ii) the intracellular Ca^{2+} concentration at equilibrium (180 nM in LCLC 103H cells (27) and 50 nM in COS 7 cells) (Fig. 3*B*).

Calpain Activity in Living Cells—The fluorogenic peptide substrate Suc-LLVY-amc (30) was used to investigate calpain activity *in vivo* after calcium stimulation. The cells were treated with 160 μM Suc-LLVY-amc and 2 μM ionomycin, and fluorescence at 460 nm was measured in 5-min intervals for up

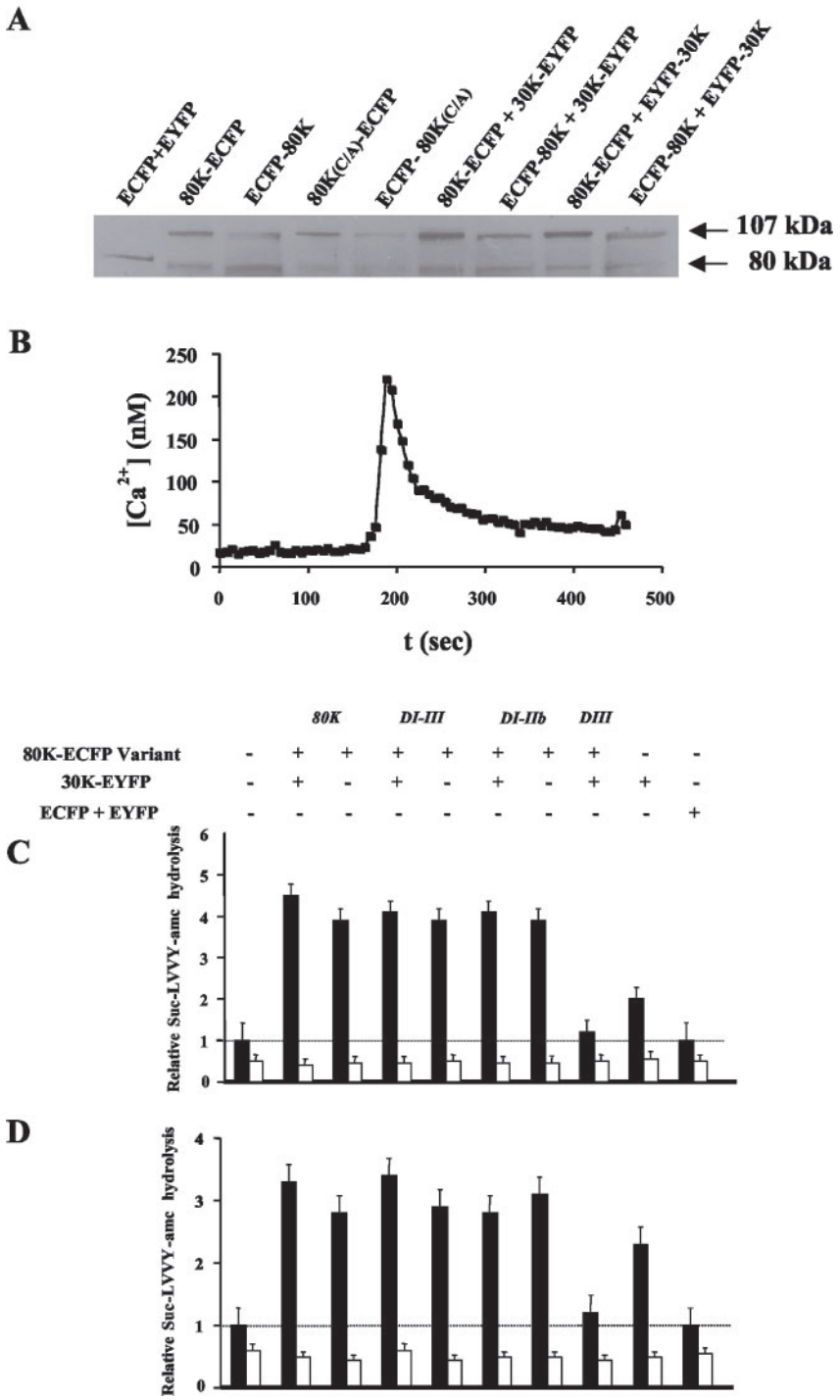

FIG. 3. **Overexpressed chimeras of human μ-calpain are Ca^{2+}-activable.** *A*, Western blots of cytoplasmic fraction of cells expressing the indicated variants probed with anti-DII antibody. The molecular masses of 80K-ECFP and ECFP-80K (107 kDa) or the large subunit of endogenous human μ-calpain (80 kDa) are indicated with *arrows*. *B*, increase of intracellular calcium concentration upon ionomycin addition to COS 7 cells. The cells were loaded with Fura-2 for 30 min and then treated with 2 μM ionomycin as explained under "Experimental Procedures." The average calcium concentration in five different cells is represented (*black squares*). *C* and *D*, calpain activity in COS 7 (*C*) and LCLC 103H cells (*D*) transiently overexpressing fluorescence-tagged variants of human μ-calpain subunits. Relative increase of Suc-LLVY-amc hydrolyzing activity compared with wild type cells (activity = 1, *dotted lines*) is shown by *black* (for cells that were not treated with AC27P) or *white bars* (cells preincubated with 50 μM AC27P), respectively. The standard deviations of three measurements are indicated (*bars*).

to 1 h. We have previously shown that the addition of the calcium ionophore results in an ~2-fold increase in calpain activity, which was specifically inhibited by AC27P (27). We have now confirmed that calpain activity was stimulated by the addition of ionomycin in both COS 7 (Fig. 3*C*) and LCLC 103H cells (Fig. 3*D*), also in agreement with previous reports in other cell lines (31–33). Furthermore, the cells overexpressing μ-calpain chimeras that include the catalytic domain showed similar levels of Ca^{2+}-dependent activity as variants of full-length 80K. Calpain activities of these fusion proteins were ~4-fold (in COS 7 cells) or ~3-fold higher (in LCLC 103H cells) than those of wild type and mock transfected cells. Most of the ionophore-induced hydrolytic activity was inhibited by preincubation of cells with the specific calpain inhibitor, 50 μM AC27P (Fig. 3, *C* and *D*), thus confirming that the observed activity results almost exclusively from calpain activation. No significant differences in activity were detected between cells co-expressing large and small subunit variants and those transfected with the large subunit chimeras alone. Interestingly, the cells that exclusively overexpressed the small subunit variants showed significantly higher hydrolytic activities than wild type and mock transfected cells.

Subcellular Localization of Human μ-Calpain Variants and Calpain Subunit Interactions—Epifluorescence microscopy was used to study (i) the localization of overexpressed μ-calpain subunits and truncated variants of the large subunit and (ii) the interaction between large and small calpain subunits *in vivo*. Both under resting and activated conditions (Fig. 4*A*), the

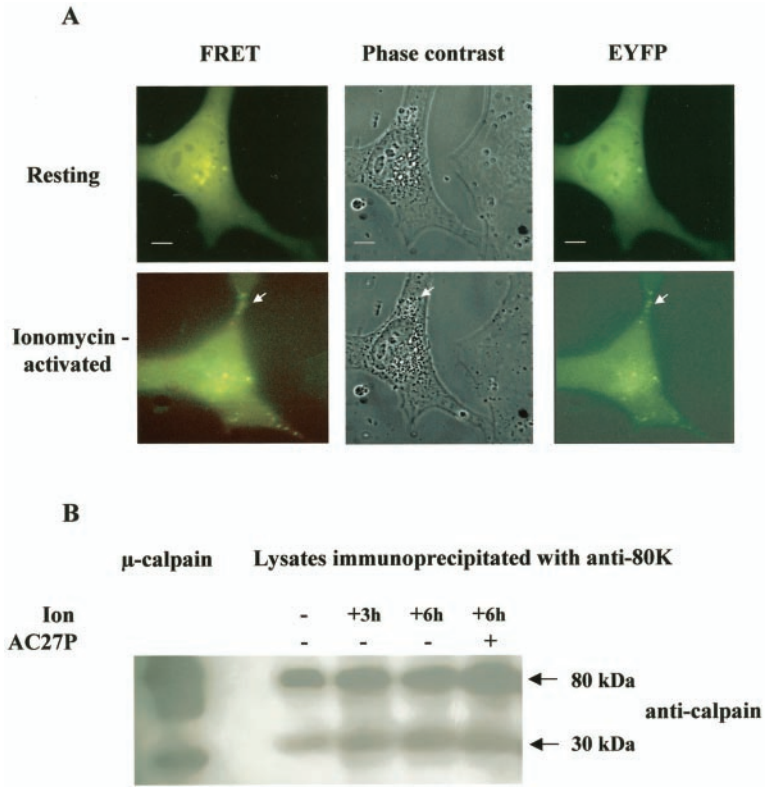

FIG. 4. **Calpain subunits associate under resting and ionomycin-activated conditions.** *A*, fluorescence analysis of COS 7 cells overexpressing large and small calpain subunits. Fluorescence channels detected FRET (*left panels*) and EYFP (*right panels*); phase contrast images are shown in the *middle panels*. Images of the same cell were taken under resting and activated conditions as indicated. The *white arrows* mark the observed fluorescence accumulation at the plasma membrane. The *bars* represent 5 μm. *B*, endogenous calpain subunits do not dissociate under calcium-activated conditions. Cytoplasmic proteins extracted from wild type LCLC 103H cells were immunoprecipitated with anti-80K antibody and detected by Western blots using anti-calpain antibody. *Ion*, cells were treated with 2 μM ionomycin for the indicated time; *AC27P*, cells were preincubated with 50 μM AC27P for 1 h and then treated with 2 μM ionomycin for the indicated time as explained under "Experimental Procedures."

80K and 30K subunits co-localized in the cytosol, as indicated by the fluorescence (colored *yellow-brown*) observed upon excitation with the FRET filter (Fig. 4*A*). Upon the addition of the ionophore the two subunits seem to migrate together, mainly to the plasma membrane (Fig. 4*A*, *white arrows*). In cells co-expressing nonfused ECFP and EYFP, we observed uniform patterns of cytoplasmic localization but no quenching of the ECFP fluorescence either under resting or activated conditions (data not shown), thus ruling out that the observed FRET effects were due to unspecific interactions. These results were corroborated by co-immunoprecipitation of the 30K and 80K subunits under resting and Ca^{2+}-activated conditions (Fig. 4*B*). No FRET was observed in cells transiently co-expressing truncated variants of μ-calpain large subunit fused to ECFP and 30K-EYFP (data not shown), in agreement with the severely reduced interaction interfaces after deletion of either the C-terminal domains (chimeras of DI-III and DI-IIb) or both the N- and C-terminal domains (DIII; compare Fig. 1, *A–D*).

Confocal laser scanning microscopy was further used to study the intracellular localization and trafficking of the μ-calpain subunits and of truncated variants thereof. Chimeras 80K-ECFP and 30K-EYFP homogenously co-localized in the cytoplasm under resting conditions, without obvious accumulation in subcellular organelles. Further, we could confirm their migration to membranes upon the addition of ionomycin (Fig. 5, *A–C*). Again, comparison of both fluorescence patterns provides additional evidence that the two subunits co-localize throughout (Fig. 5*C*). The migration of the small subunit variant seems to occur in vesicle-like structures of about 1 μm in diameter (Fig. 5*B*). Whether the large subunit is included within these structures is unknown, but co-localization of both subunits throughout would point to its inclusion in these vesicles (see "Discussion").

Overexpressed ECFP-DI-III was distributed homogenously in the cytoplasm and within the nucleus (Fig. 5*D*). In this figure, images corresponding to the same cell are shown at two different levels (whole cell, *upper panels*; nucleus, *lower panels*) to highlight the ionomycin-dependent migration of ECFP-DI-III to both the plasma and nuclear membranes. In contrast, overexpressed ECFP-DI-IIb was mainly observed in the cell nucleus including the nucleoli, and this localization pattern did not change after the addition of ionomycin (Fig. 5*E*).

To confirm the plasma membrane association of calpain or its subunits, 80K and DI-III DNAs were fused to EYFP and supertransfected into LCLC 103H clone cells constitutively expressing a membrane marker, mem-ECFP. Fluorescence image series were taken in the respective channels, processed by deconvolution algorithms, and analyzed comparatively pixel-by-pixel with a co-localization program. The result of this process is given by a representative example of the 80K-EYFP construct (Fig. 6); it clearly demonstrates the plasma membrane association of the 80K subunit. Experiments conducted with the DI-III construct had similar outcomes (data not shown).

Subcellular Localization of Calpain Variants by Western Blot Analysis—To further confirm the results obtained with microscopic techniques, the relative distribution of calpain chimeras in transfected LCLC 103H cells was assessed via Western blot analysis. Equal amounts of cells (10^6) either untreated or incubated with 2 μM ionomycin were fractionated by centrifugation. The purity of isolated fractions was verified by measuring a ~15-fold higher activity of lactate dehydrogenase in the cytoplasmic than in the nuclear fractions (data not shown), indicating a successful separation (34). Moreover, only the nuclear but not the cytoplasmic fraction was stained by propidium iodide (data not shown).

The separated fractions were analyzed by Western blot using either anti-DII or a polyclonal antibody that recognizes the fused fluorescent proteins, anti-living colors. The human μ-calpain large subunit was detected in the cytoplasmic, membrane, and nuclear fractions of cells overexpressing 80K-ECFP before and after ionomycin addition (Fig. 7*A*). After ionomycin treatment, however, the relative amount of calpain large subunit variant in the membrane fractions increased substantially. In

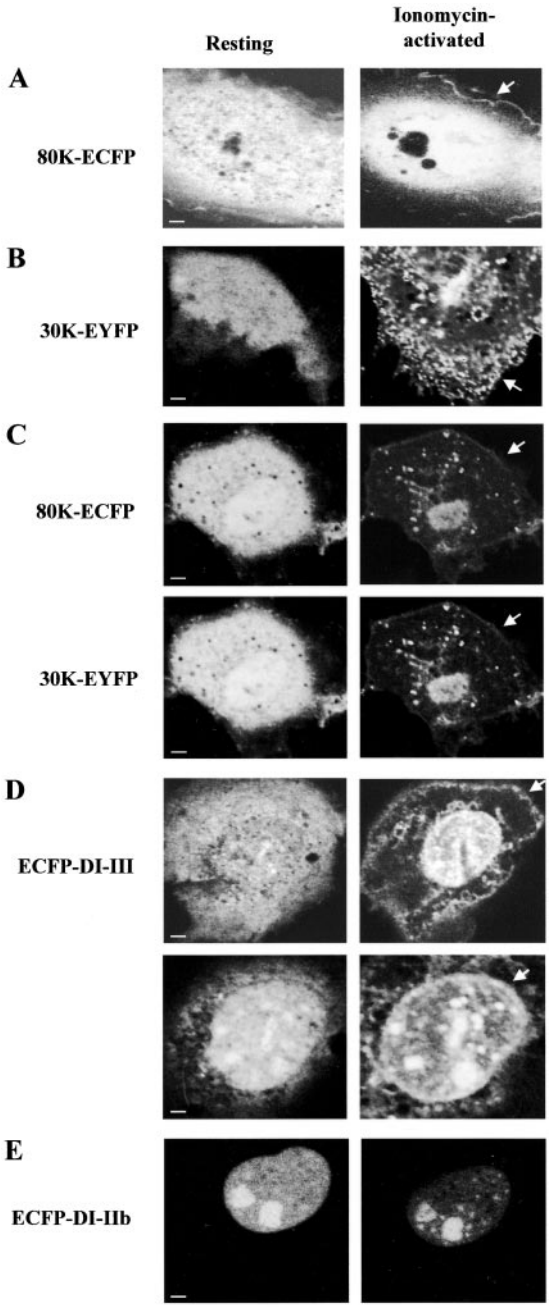

FIG. 5. **Intact and truncated variants of the μ-calpain subunits show different subcellular localization.** Confocal images of COS 7 cells overexpressing 80K-ECFP (*A*), 30K-EYFP (*B*), 80K-ECFP and 30K-EYFP (*C*, leakage from ECFP in EYFP has been corrected), ECFP-DI-III (*D*, *upper* and *lower panels* show the whole cell or the cell nucleus, respectively), and ECFP-DI-IIb (*E*, both images show the cell nucleus). The fluorescence channel detected ECFP, except in *B* and *C* (*lower images*), where EYFP has been detected. The images were taken under resting (*left column*) and activated (*right column*) conditions. Series of images with a distance of 50 μm were taken for each channel using single-band emission filters. Notice the increased fluorescence at the plasma membrane of ionomycin-treated cells (*white arrows* in *A–D*), indicating ionomycin-dependent migration to the membrane. The *bars* represent 2.5 μm (*A*), 5 μm (*B*, *left panel*; *C*; *D*, *upper panel*; and *E*) and 1 μm (*B*, *right panel*, and *D*, *lower panel*).

the cytoplasmic fraction of resting cells overexpressing ECFP, a faint band corresponding to endogenous calpain was detected, which disappeared in activated cells because of autolysis (data not shown). Unexpectedly, the intensity of the 80-kDa band, corresponding to endogenous calpain, was increased in cells overexpressing the chimeric 80K-ECFP form, compared with wild type cells. This feature may reflect the existence of an uncharacterized mechanism(s) of up-regulation of calpain expression by its isolated subunits, also suggested by the results of activity measurements (Fig. 3, *C* and *D*).

The truncated variant, ECFP-DI-III, was primarily detected in the nucleus of the cells, but it was also detectable in the cytoplasmic fraction (Fig. 7*B*). After ionomycin addition, this large subunit variant was enriched in the membrane fractions as well. In striking contrast, ECFP-DI-IIb was localized mainly in the nuclear and nucleolar fractions and did not relocalize after ionophore treatment (Fig. 7*C*).

Domain DIII Contributes to Membrane Targeting of Calpain—We had determined that chimeric variants of μ-calpain that contain domain DIII were targeted to membranes upon ionomycin-mediated activation. Considering also the proposed membrane targeting role of DIII (14), we investigated the intracellular localization of overexpressed ECFP-DIII, as well as possible interactions between the ECFP-DIII/30K-EYFP pair in COS 7 and LCLC 103H cells. The chimeric protein ECFP-DIII was primarily localized in the cytoplasmic fraction, but it was also detectable in the membrane fraction in resting cells (Fig. 7*D*). After the addition of ionomycin, ECFP-DIII was enriched in the membrane fraction (Fig. 7*D*).

N-terminal Helices in Domain DI Are a Putative Nuclear Targeting Motif—Ubiquitous calpains lack stretches of positively charged residues like those of the SV40 large tumor antigen ($PKKKRKV^{132}$) (35) or the protooncogene c-*myc* (PAAKRVKLD) (36), which have been repeatedly implicated as nuclear localization signals (recently reviewed in Ref. 37). The nuclear and nucleolar localization of the truncated ECFP-DI-IIb variant was therefore unanticipated and provoked an investigation regarding structural elements that could be responsible for this finding. With this aim, we produced five additional chimeras derived from this variant and overexpressed them in LCLC 103H cells to perform subcellular localization studies similar to those described above. The selected chimeras either lack the two helices within the N-terminal DI and the linker to DIIa (ECFP-Δ(Ser^2–Leu^{55})DI-IIb) or have positively charged residues within this domain replaced by a helix-disrupting proline within the first (ECFP-[K20P]DI-IIb) or the second helix (ECFP-[R48P]DI-IIb). An additional charge-mutated variant had two consecutive basic residues in domain DIIb, Arg^{376} and Arg^{377}, replaced by alanines (ECFP-[R376A,R377A]DI-IIb). Finally, a chimera consisting of the N-terminal helices fused to the N terminus of ECFP was constructed (ECFP-(Ser^2–Leu^{55})).

To clearly document their subcellular localization, we transfected these constructs into a LCLC 103H cell clone that constitutively expresses histone H2A fused to EYFP (Fig. 8), enabling us to study the possible influence of the mutated calpain DI-IIb constructs on nuclear morphology and chromatin structure. Already within 24 h post-transfection the chromatin segregated, with chromatin clusters appearing at the inner nuclear envelope. The morphology of nuclei changed dramatically from slightly indented to multilobed "kidney" forms (Fig. 8*C*). Interestingly, with the exception of the ECFP-[R376A, R377A]DI-IIb chimera, all of the investigated variants accumulate in the cell nucleus (Fig. 8). Deletion of both helices, however, diminished the nuclear localization of DI-IIb. The overexpressed chimeric proteins do not appear within organelles (endoplasmic reticulum and vesicles). These findings suggest an important role for the N-terminal helices of DI in the nuclear localization of ubiquitous calpains.

DISCUSSION

Differential Subcellular Distribution of Ubiquitous Calpains and Calpastatin—It is becoming increasingly clear that ubiq-

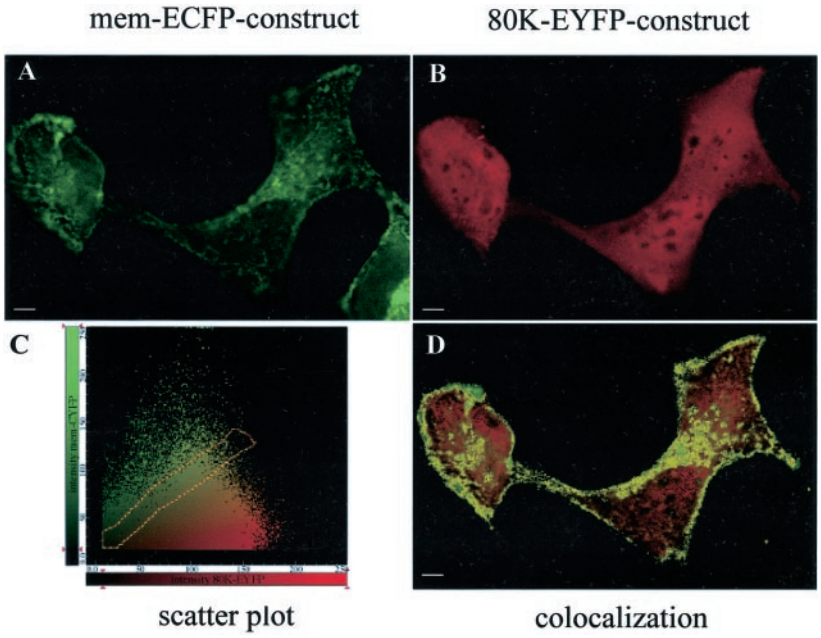

FIG. 6. **Co-localization of 80K-EYFP and mem-ECFP in LCLC 103H cells.** Cells of a clone constitutively expressing mem-ECFP were supertransfected with 80K-EYFP DNA. Fluorescence microscopical analysis was performed 2 days post-transfection in ionomycin-activated cells. Series of images were taken in 500-nm distances for both channels, alternatively, subsequently processed by deconvolution algorithms, and a color look-up table was applied to the central image choosing *green* and *red* for ECFP and EYFP, respectively. The results are given in *A* and *B*. These images were analyzed pixel-by-pixel for co-localization. The result of this analysis is shown in the scatter plot (*C*). According to theory co-localization events are located in the line $x = y$. An area around this line was selected (surrounded by the *dotted line*). The pixels of this area are overlaid in *yellow* on the merged reconstruction of the original images (co-localization image, *D*). The *bars* represent 5 μm. Co-localization of 80K-EYFP and mem-ECFP is very prominent in the plasma membrane.

uitous calpains play important physiological roles *in vivo* (see for instance Ref. 38) and are implicated in pathological processes such as ischemia/reperfusion injury (39, 40). The mechanisms of calpain assembly, activation, and regulation as well as of cellular trafficking are therefore of considerable interest, but they are only scarcely understood. Here we have investigated the activation mechanism of ubiquitous calpains *in vivo*, in particular the subcellular localization of calpain subunits and their interaction under resting and Ca^{2+}-activated conditions.

The addition of 2 μM ionomycin increased the intracellular Ca^{2+} level (Fig. 3*B* and Ref. 27), and this moderate increase in Ca^{2+} concentration activates endogenous calpains in the two cell lines studied (Fig. 3, *C* and *D*). We had previously shown that calpain activation triggers the intrinsic apoptotic pathway, with the first signals of caspase activity detected 3 h after ionomycin treatment (27). The ionomycin concentration employed in the current investigation, however, did not cause cytotoxic effects on wild type cells up to 30 min (data not shown), the time period during which the microscopic localization experiments were carried out. Thus, all of the observations discussed below relate to cells before the onset of apoptosis.

We have detected a differential distribution of calpains and calpastatin in LCLC 103H cells. Although calpains are distributed homogenously in the cytoplasm, their endogenous inhibitor, calpastatin, was localized not only in the cytoplasm but also in the cell nucleus. Of particular note, we detected ionomycin-induced redistribution of calpain toward membranes, whereas the nuclear localization of calpastatin was unaffected by the increase in intracellular Ca^{2+} concentration. Similar results have also been documented in proliferating culture cells using immunofluorescent light microscopy (41). Although calpains are usually viewed as cytoplasmic enzymes (Fig. 2, *A* and *B* and Ref. 42), they have also been detected in the nucleus of C-33A cervical carcinoma cells (41, 43). In contrast, calpastatin is mainly localized in the nucleus (Fig. 2*C*; see also Ref. 41) or in nuclear invaginations (44). Active transport of fluorescein-labeled μ-calpain to the nucleus has been reported, whereas labeled m-calpain and calpastatin were poorly transported at best (45). Our results corroborate the variable distribution of calpain and calpastatin in different human cells (41) but in particular stress the physical separation between calpains and their endogenous protein inhibitor.

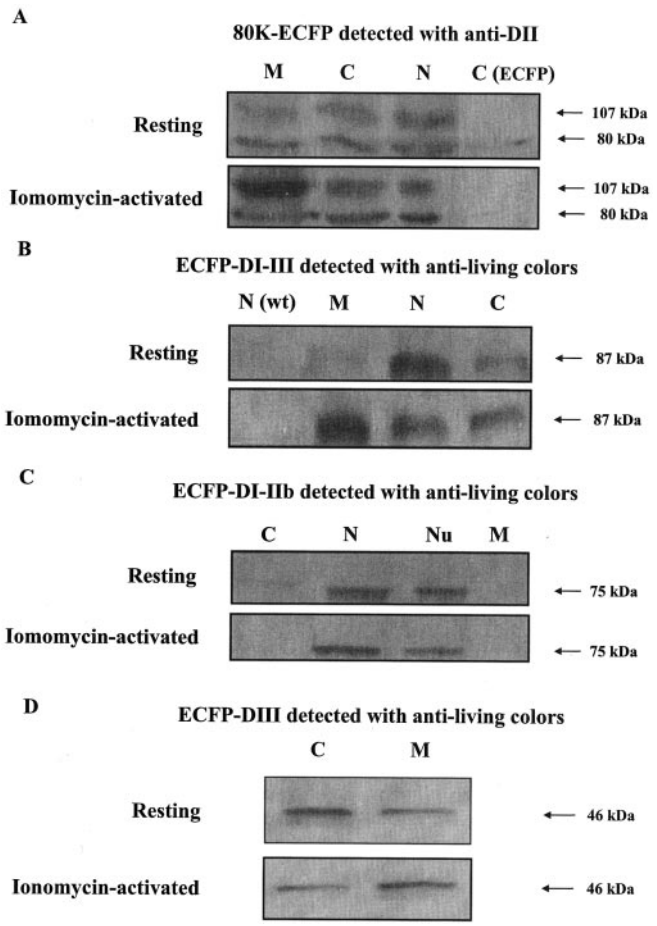

FIG. 7. **The synaptotagmin C2-like domain of human μ-calpain contributes to membrane targeting.** Western blot analysis of subcellular fractions of COS 7 cells overexpressing fluorescence-tagged calpain variants 80K-ECFP (*A*), ECFP-DI-III (*B*), ECFP-DI-IIb (*C*), and ECFP-DIII (*D*). Molecular masses of the variants (107, 87, 75, and 46 kDa, respectively) are indicated on the *right*. Blotted proteins were detected with antibodies anti-DII (*A*) or anti-living colors (*B–D*). *C*, cytoplasmic; *M*, membrane; *N*, nuclear; *Nu*, nucleolar. *Upper panels*, untreated cells; *lower panels* (*Ionomycin-activated*), cells treated with 2 μM ionomycin; *ECFP*, lysates from cells overexpressing ECFP; *wt*, wild type COS 7 cells.

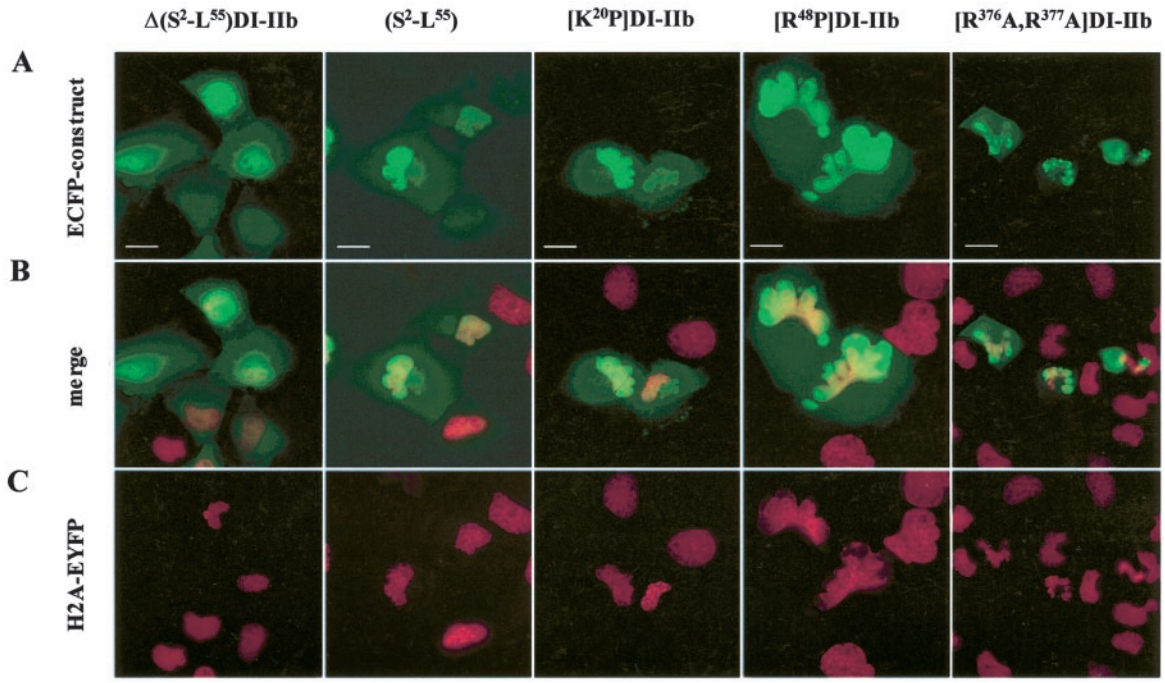

FIG. 8. **N-terminal domain DI of human μ-calpain as nuclear targeting motif.** Subcellular localization by fluorescence microscopy of ECFP-DI-IIb variants, ECFP-Δ(Ser²–Leu⁵⁵)DI-IIb, ECFP-(Ser²–Leu⁵⁵), ECFP-[K20P]DI-IIb, ECFP-[R48P]DI-IIb, and ECFP-[R376A,R377A]DI-IIb, overexpressed in a LCLC 103H clone expressing constitutively histone H2A coupled to EYFP. *A*, expression pattern of the respective fragment in the ECFP-channel (*green*). *C*, expression pattern of histone H2A in the EYFP channel (*red*); *B*, merged expression patterns (*A* and *C*). Series of images with a distance of 200 nm were taken for each channel using single-band emission filters, processed by volume deconvolution and false colorized (ECFP = *green*; EYFP = *red*) before merging. For the final presentation the images were contrast-enhanced by a logarithmic function to strengthen the weak intensities in the cytoplasm. The *bars* represent 25 μm (Δ(Ser²–Leu⁵⁵)DI-IIb, [R376A,R377A]DI-IIb), 20 μm ((Ser²–Leu⁵⁵), [K20P]DI-IIb), and 13 μm ([R48P]DI-IIb).

Calpain Subunits Do Not Dissociate upon Activation—The hypothesis that calpain subunits dissociate in the presence of Ca^{2+} has previously been tested *in vitro* using techniques that cannot avoid interference from Ca^{2+}-induced aggregation phenomena and/or that are probably obscured by large subunit autolysis (1, 46). To overcome these limitations and to study for the first time the interaction between calpain subunits *in vivo*, we developed a strategy based on FRET visualization between fluorescence-tagged calpain subunits.

First we verified that all of the ECFP fusion proteins that contain the catalytic subunit were enzymatically active, as shown by cleavage of the cell-permeable small peptide substrate Suc-LLVY-amc (Fig. 3, *C* and *D*). These activities were Ca^{2+}-dependent, independent of the position of the fluorescence label, and were reduced to the level of the endogenous background activity in control cells preincubated with AC27P. In our hands, the minimum active μ-calpain fragment comprises residues Ser²–Thr³⁹⁰ (variant DI-IIb), in agreement with recent results (15, 47). Thus, domains DIII and DIV are dispensable for calpain activity on small peptide substrates, although they could play roles in enzyme localization and protein substrate recognition, as suggested (14). Surprisingly, not only cells overexpressing the 80K catalytic subunit alone but also those that exclusively overexpress the 30K regulatory subunit showed significantly higher Ca^{2+}-induced activities than wild type and mock transfected cells. This observation points to a previously unanticipated cross-talk between the two calpain subunits, which results in up-regulation of the 80K by the 30K subunit and vice versa. In this regard, we have observed that down-regulation of the m- or μ-calpain catalytic subunit results in a concomitant decrease in the levels of the regulatory subunit.[4] The association and stabilization of the exogenous 30K subunit with endogenous m-/μ-calpain 80K subunits and vice versa could contribute to the observed effect.

Because of their higher overexpression levels, variants 80K-ECFP, ECFP-DI-III, ECFP-DI-IIb, ECFP-DIII, and 30K-EYFP were selected for subunit interactions studies. We only observed the FRET effect in cells co-expressing 80K-ECFP and 30K-EYFP, both under resting and Ca^{2+}-activated conditions. This observation, together with the results of immunoprecipitation experiments conducted with endogenous calpains, indicates that under the given experimental conditions the subunits of μ-calpain associate not only under resting conditions but also after activation. Domain IV seems to be indispensable in subunit interaction because we could not detect energy transfer between the small subunit and variants of the large subunit lacking DIV.

These results are in agreement with several previous findings *in vitro*: (i) Both subunits of m-/μ-calpain were co-precipitated by monoclonal antibodies directed against each single subunit in the presence of Ca^{2+} concentrations supporting catalytic activity (12). (ii) The 80K subunit alone lacks proteinase activity *in vitro*, even in the presence of Ca^{2+}, but Ca^{2+}-dependent calpain activity is observed following association of the two subunits (48). (iii) Subunit exchange does not occur in mixtures of wild type and [C105S]80K rat m-calpain in the presence of Ca^{2+} (11). (iv) His-tagged rat [C105S]80K m-calpain does not dissociate in the presence of Ca^{2+} (49). (v) Natural bovine m-calpain, after irreversible inhibition with z-LLY-CHN_2, bound to immobilized casein and was eluted as a

[4] S. Gil-Parrado, T. Tannenberg, L. Ruiz-Heinrich, O. Popp, and C. Sommerhof, manuscript in preparation.

heterodimer. (vi) Finally, the crystal structures of m-calpain disclose large (~3,000 Å^2) interaction interfaces between large and small subunits.

Despite this overwhelming body of evidence in support of the indivisibility of the calpain heterodimer, some authors have argued that both calpain subunits are only loosely associated and therefore prone to dissociation. For instance, it was suggested that the small subunit is exclusively needed to assist folding of the 80K subunit. Along these lines, it has been reported that dissociation of the large subunit from the small subunit on exposure to Ca^{2+} was required for the expression of activity. Moreover, the 80K subunit shows a calcium sensitivity identical to that of the activated form of calpain but not of the original control calpain (50). In a recent report, Pal and coworkers (46) discuss the results of crystallization trials conducted with Ca^{2+}-activated m-calpain. Crystals were grown that contained only the 30K subunit, whereas the large subunit was largely found as an amorphous precipitate. However, these results were obtained with samples maintained for large periods of time at the nonphysiologically high protein and calcium concentrations needed for crystallization.

In contrast, the current studies were performed under cytosolic calcium and protein concentrations and are at odds with the possibility of subunit dissociation *in vivo*. Of course, we cannot completely exclude reversible dissociation in a time scale much lower than the observation time and/or as a minor process, but dissociation of calpain subunits seems to be unlikely according to our current results and functional and structural evidence cited above.

Calpain Autolysis Products Are Not Detected in Vivo—Calpain autolysis *in vitro* has been repeatedly reported (51, 52). These results seeded the speculation that calpain autolysis could contribute to the differential subcellular targeting of the enzyme, for instance via dissociation of truncated subunits. Antibodies raised against the N-terminal peptide of the 80K subunit, Ser^2–Gln^{21} (anti-peptide 80K), recognize the intact (dissociated) large subunit in Western blots of purified calpain and in cytoplasmic extracts (Ref. 51 and data not shown). In a similar manner, antibodies raised against peptide Leu^{28}–Asn^{33} (anti-peptide 76K) recognize 76- and 40-kDa autolysis fragments *in vitro*. However, these anti-peptide antibodies failed to detect the catalytic subunit or its 76/40-kDa N-terminal autolysis products in living cells, both under resting and under activated conditions. Either these antibodies are not sensitive enough for immunocytofluorescence studies, or these fragments are not produced *in vivo*. Alternatively, the N-terminal region of the 80K subunit may not be accessible to these antibodies within the heterodimeric calpain molecule *in vivo* or may adopt a conformation(s) that differs from the one(s) recognized by these antibodies. Regardless, additional experimental evidence presented here excludes unrestricted degradation of calpain in our current setting. We cannot rule out, however, that autolysis at the N terminus of both subunits and other sites could occur in other cell lines and/or in different experimental settings, with concomitant dissociation of calpain subunits (53). This might in turn affect the differential intracellular distribution of the protease, allowing calpainolysis to take place, *e.g.* in the nuclei (54–57).

Nuclear Localization of Variant DI-IIb—ECFP-DI-IIb was almost exclusively localized in the nucleus and nucleoli (Fig. 5*E*). It seems unlikely that simple diffusion through nuclear pores is responsible for this localization, because the variants ECFP, EYFP, ECFP-DIII, and 30K-EYFP, which are of similar size or smaller, are distributed homogenously in the cytoplasm and nucleus.

The three-dimensional structure of m-calpain reveals a positively charged region at the N terminus of the large subunit comprising two α-helices (Fig. 1, *A–E*), one of which is largely solvent-exposed in m-calpain and by analogy in all analyzed μ-calpain variants containing the homologous N-terminal peptide stretch (Fig. 1*F*). Recently, positively charged helical structures have been found responsible for nuclear targeting of several unrelated proteins (58–60). In the light of these findings and considering the lack of a consensus sequence for nuclear localization in ubiquitous calpains, we speculated that the α-helices at the N terminus of the large subunit were important for nuclear targeting. Indeed, deletion of both helices from the DI-IIb chimera results in a form that is localized mainly in the cytoplasm, whereas the helices alone were able to direct ECFP to the cell nucleus. Our data and reports of calpain involvement in signaling pathways (38, 61) suggest that the nucleo-cytoplasmic distribution of calpains may be altered in response to cell activation, differentiation, stress, or other stimuli.

Domain III Is Critical for Membrane Targeting of μCP—The overexpressed catalytic subunit and its truncated variants, DI-III and DIII, migrated to cell membranes under activating conditions, in agreement with previous reports (62, 63). In contrast, ECFP-DI-IIb did not migrate to membranes, indicating a critical role of the synaptotagmin C2-like domain DIII in the membrane targeting mechanism of calpains. This finding is in line with the Ca^{2+}-dependent phospholipid binding ability of the isolated domain *in vitro* (20). Further, we detected relocalization of the overexpressed light chain chimera 30K-EYFP upon ionomycin addition. Remarkably, redistribution of this form was associated with the formation of organized structures, possibly vesicles (Fig. 5*B*). This suggests that 30K small subunit could oligomerize in the absence of the large subunit, as observed by others *in vitro* (46).

In summary, we provide insight into the mechanisms of calpain assembly, activation, and regulation *in vivo*. Our results suggest that calpain activity in the cells is regulated not only by calpastatin but also by differential intracellular localization and in particular membrane targeting of activated calpain. Dissociation of its intact subunits, in contrast, appears to play at most a secondary role in its regulation. Further, we have begun to unravel the roles of noncatalytic domains for calpain activity *in vivo*. Most interestingly, we confirm and extend results implicating the synaptotagmin C2-like domain III as well as the light chain domains in membrane targeting. In addition, we identify a putative novel role for the N-terminal domain I, regulation of nuclear localization.

Acknowledgments—We are grateful to Mathias Hafner for facilitating intracellular activity and calcium measurements and to Axel Ullrich and Axel Choidas for valuable suggestions. We also thank Dusica Gabrijelcic-Geiger for providing anti-calpain antibody. Claudia Huber, Barbara Meisel, and Anna Heckel-Pompey are acknowledged for excellent technical assistance.

REFERENCES

1. Suzuki, K., and Sorimachi, H. (1998) *FEBS Lett.* **433,** 1–4
2. Ohno, S., Emori, Y., Imajoh, S., Kawasaki, H., Kisaragi, M., and Suzuki, K. (1984) *Nature* **312,** 566–570
3. Sakihama, T., Kakidani, H., Zenita, K., Yumoto, N., Kikuchi, T., Sasaki, T., Kannagi, R., Nakanishi, S., Ohmori, M., Takio, K., Titani, K., and Murachi, T. (1985) *Proc. Natl. Acad. Sci. U. S. A.* **82,** 6075–6079
4. Dayton, W. R., Schollmeyer, J. V., Lepley, R. A., and Cortes, L. R. (1981) *Biochim. Biophys. Acta* **659,** 48–61
5. Shiraha, H., Glading, A., Chou, J., Jia, Z., and Wells, A. (2002) *Mol. Cell. Biol.* **22,** 2716–2727
6. Yamato, S., Tanaka, K., and Murachi, T. (1983) *Biochem. Biophys. Res. Commun.* **115,** 715–721
7. Cong, M., Thompson, V. F., Goll, D. E., and Antin, P. B. (1998) *J. Biol. Chem.* **273,** 660–666
8. Salvesen, G., Parkes, C., Abrahamson, M., Grubb, A., and Barrett, A. J. (1986) *Biochem. J.* **234,** 429–434
9. Benetti, R., Del Sal, G., Monte, M., Paroni, G., Brancolini, C., and Schneider, C. (2001) *EMBO J.* **20,** 2702–2714
10. Saido, T. C., Nagao, S., Shiramine, M., Tsukaguchi, M., Sorimachi, H.,

Murofushi, H., Tsuchiya, T., Ito, H., and Suzuki, K. (1992) *J. Biochem.* (*Tokyo*) **111,** 81–86
11. Dutt, P., Arthur, J. S., Croall, D. E., and Elce, J. S. (1998) *FEBS Lett.* **436,** 367–371
12. Zhang, W., and Mellgren, R. L. (1996) *Biochem. Biophys. Res. Commun.* **227,** 891–896
13. Hosfield, C. M., Elce, J. S., Davies, P. L., and Jia, Z. (1999) *EMBO J.* **18,** 6880–6889
14. Strobl, S., Fernandez-Catalan, C., Braun, M., Huber, R., Masumoto, H., Nakagawa, K., Irie, A., Sorimachi, H., Bourenkow, G., Bartunik, H., Suzuki, K., and Bode, W. (2000) *Proc. Natl. Acad. Sci. U. S. A.* **97,** 588–592
15. Moldoveanu, T., Hosfield, C. M., Lim, D., Elce, J. S., Jia, Z., and Davies, P. L. (2002) *Cell* **108,** 649–660
16. Blanchard, H., Li, Y., Cygler, M., Kay, C. M., Simon, J., Arthur, C., Davies, P. L., and Elce, J. S. (1996) *Protein Sci.* **5,** 535–537
17. Dutt, P., Arthur, J. S., Grochulski, P., Cygler, M., and Elce, J. S. (2000) *Biochem. J.* **348,** 37–43
18. Mellgren, R. L. (1987) *FASEB J.* **1,** 110–115
19. Suzuki, K., Imajoh, S., Emori, Y., Kawasaki, H., Minami, Y., and Ohno, S. (1987) *FEBS Lett.* **220,** 271–277
20. Tompa, P., Emori, Y., Sorimachi, H., Suzuki, K., and Friedrich, P. (2001) *Biochem. Biophys. Res. Commun.* **280,** 1333–1339
21. Horikawa, Y., Oda, N., Cox, N. J., Li, X., Orho-Melander, M., Hara, M., Hinokio, Y., Lindner, T. H., Mashima, H., Schwarz, P. E., del Bosque-Plata, L., Oda, Y., Yoshiuchi, I., Colilla, S., Polonsky, K. S., Wei, S., Concannon, P., Iwasaki, N., Schulze, J., Baier, L. J., Bogardus, C., Groop, L., Boerwinkle, E., Hanis, C. L., and Bell, G. I. (2000) *Nat. Genet.* **26,** 163–175
22. Selvin P. R. (2000) *Nat. Biotechnol.* **7,** 730–734
23. Manders, E. M. M., Verbeek, F. J., and Aten, J. A. (1993) *J. Microsc.* **169,** 375–382
24. Bestvater, F., Knoch, T. A., Langowski, J., and Spiess, E. (2002) *BioTechniques* **32,** 844, 846, and 848–850
25. Muramatsu, M., Hayashi, Y., Onishi, T., Sakai, M., and Takai, K. (1974) *Exp. Cell Res.* **88,** 245–251
26. Smith, P. K., Krohn, R. I., Hermanson, G. T., Mallia, A. K., Gartner, F. H., Provenzano, M. D., Fujimoto, E. K., Goeke, N. M., Olson, B. J., and Klenk, D. C. (1985) *Anal. Biochem.* **150,** 76–85
27. Gil-Parrado, S., Fernandez-Montalvan, A., Assfalg-Machleidt, I., Popp, O., Bestvater, F., Holloschi, A., Knoch, T. A., Auerswald, E. A., Welsh, K., Reed, J. C., Fritz, H., Fuentes-Prior, P., Spiess, E., Salvesen, G. S., and Machleidt, W. (2002) *J. Biol. Chem.* **277,** 27217–27226
28. Yamazaki, T., Haass, C., Saido, T. C., Omura, S., and Ihara, Y. (1997) *Biochemistry* **36,** 8377–8383
29. Guttmann, R. P., and Johnson, G. V. (1998) *J. Biol. Chem.* **273,** 13331–13338
30. Bronk, S. F., and Gores, G. J. (1993) *Am. J. Physiol.* **264,** G744–G751
31. Kavita, U., and Mizel, S. B. (1995) *J. Biol. Chem.* **270,** 27758–27765
32. Norris, F. A., Atkins, R. C., and Majerus, P. W. (1997) *J. Biol. Chem.* **272,** 10987–10989
33. Schoenwaelder, S. M., Yuan, Y., Cooray, P., Salem, H. H., and Jackson, S. P. (1997) *J. Biol. Chem.* **272,** 1694–1702
34. Martins, L. M., Kottke, T., Mesner, P. W., Basi, G. S., Sinha, S., Frigon, N., Jr., Tatar, E., Tung, J. S., Bryant, K., Takahashi, A., Svingen, P. A., Madden, B. J., McCormick, D. J., Earnshaw, W. C., and Kaufmann, S. H. (1997) *J. Biol. Chem.* **272,** 7421–7430
35. Kalderon, D., Roberts, B. L., Richardson, W. D., and Smith, A. E. (1984) *Cell* **39,** 499–509
36. Makkerh, J. P., Dingwall, C., and Laskey, R. A. (1996) *Curr. Biol.* **6,** 1025–1027
37. Jans, D. A., Xiao, C. Y., and Lam, M. H. (2000) *Bioessays* **22,** 532–544
38. Glading, A., Lauffenburger, D. A., and Wells, A. (2002) *Trends Cell Biol.* **12,** 46–54
39. Chen, M., He, H., Zhan, S., Krajewski, S., Reed, J. C., and Gottlieb, R. A. (2001) *J. Biol. Chem.* **276,** 30724–30728
40. Chen, M., Won, D. J., Krajewski, S., and Gottlieb, R. A. (2002) *J. Biol. Chem.* **277,** 29181–29186
41. Lane, R. D., Allan, D. M., and Mellgren, R. L. (1992) *Exp. Cell Res.* **203,** 5–16
42. Murakami, T., Hatanaka, M., and Murachi, T. (1981) *J. Biochem.* (*Tokyo*) **90,** 1809–1816
43. Reville, W. J., Goll, D. E., Stromer, M. H., Robson, R. M., and Dayton, W. R. (1976) *J. Cell Biol.* **70,** 1–8
44. Averna, M., De Tullio, R., Salamino, F., Melloni, E., and Pontremoli, S. (1999) *FEBS Lett.* **450,** 13–16
45. Mellgren, R. L., and Lu, Q. (1994) *Biochem. Biophys. Res. Commun.* **204,** 544–550
46. Pal, G. P., Elce, J. S., and Jia, Z. (2001) *J. Biol. Chem.* **276,** 47233–47238
47. Hata, S., Sorimachi, H., Nakagawa, K., Maeda, T., Abe, K., and Suzuki, K. (2001) *FEBS Lett.* **501,** 111–114
48. Graham-Siegenthaler, K., Gauthier, S., Davies, P. L., and Elce, J. S. (1994) *J. Biol. Chem.* **269,** 30457–30460
49. Elce, J. S., Davies, P. L., Hegadorn, C., Maurice, D. H., and Arthur, J. S. (1997) *Biochem. J.* **326,** 31–38
50. Yoshizawa, T., Sorimachi, H., Tomioka, S., Ishiura, S., and Suzuki, K. (1995) *Biochem. Biophys. Res. Commun.* **208,** 376–383
51. Gabrijelcic-Geiger, D., Mentele, R., Meisel, B., Hinz, H., Assfalg-Machleidt, I., Machleidt, W., Moller, A., and Auerswald, E. A. (2001) *Biol. Chem.* **382,** 1733–1737
52. Suzuki, K., Tsuji, S., Kubota, S., Kimura, Y., and Imahori, K. (1981) *J. Biochem.* (*Tokyo*) **90,** 275–278
53. Nakagawa, K., Masumoto, H., Sorimachi, H., and Suzuki, K. (2001) *J. Biochem.* (*Tokyo*) **130,** 605–611
54. Mellgren, R. L. (1991) *J. Biol. Chem.* **266,** 13920–13924
55. Hirai, S., Kawasaki, H., Yaniv, M., and Suzuki, K. (1991) *FEBS Lett.* **287,** 57–61
56. Piechaczyk, M. (2000) *Methods Mol. Biol.* **144,** 297–307
57. Pariat, M., Salvat, C., Bebien, M., Brockly, F., Altieri, E., Carillo, S., Jariel-Encontre, I., and Piechaczyk, M. (2000) *Biochem. J.* **345,** 129–138
58. Ciruela, A., Hinchliffe, K. A., Divecha, N., and Irvine, R. F. (2000) *Biochem. J.* **346,** 587–591
59. Moede, T., Leibiger, B., Pour, H. G., Berggren, P., and Leibiger, I. B. (1999) *FEBS Lett.* **461,** 229–234
60. Chen, M., Elder, R. T., Yu, M., O'Gorman, M. G., Selig, L., Benarous, R., Yamamoto, A., and Zhao, Y. (1999) *J. Virol.* **73,** 3236–3245
61. Azam, M., Andrabi, S. S., Sahr, K. E., Kamath, L., Kuliopulos, A., and Chishti, A. H. (2001) *Mol. Cell. Biol.* **21,** 2213–2220
62. Michetti, M., Salamino, F., Tedesco, I., Averna, M., Minafra, R., Melloni, E., and Pontremoli, S. (1996) *FEBS Lett.* **392,** 11–15
63. Zhao, X., Posmantur, R., Kampfl, A., Liu, S. J., Wang, K. K., Newcomb, J. K., Pike, B. R., Clifton, G. L., and Hayes, R. L. (1998) *J. Cereb. Blood Flow Metab.* **18,** 161–167